Describing strong correlation with fractional-spin correction in density functional theory

Neil Qiang Su[a], Chen Li[a], and Weitao Yang[a,b,1]

[a]Department of Chemistry, Duke University, Durham, NC 27708; and [b]Key Laboratory of Theoretical Chemistry of Environment, School of Chemistry and Environment, South China Normal University, Guangzhou 510006, China

Edited by Michael L. Klein, Temple University, Philadelphia, PA, and approved August 8, 2018 (received for review April 24, 2018)

An effective fractional-spin correction is developed to describe static/strong correlation in density functional theory. Combined with the fractional-charge correction from recently developed localized orbital scaling correction (LOSC), a functional, the fractional-spin LOSC (FSLOSC), is proposed. FSLOSC, a correction to commonly used functional approximations, introduces the explicit derivative discontinuity and largely restores the flat-plane behavior of electronic energy at fractional charges and fractional spins. In addition to improving results from conventional functionals for the prediction of ionization potentials, electron affinities, quasiparticle spectra, and reaction barrier heights, FSLOSC properly describes the dissociation of ionic species, single bonds, and multiple bonds without breaking space or spin symmetry and corrects the spurious fractional-charge dissociation of heteroatom molecules of conventional functionals. Thus, FSLOSC demonstrates success in reducing delocalization error and including strong correlation, within low-cost density functional approximation.

exchange-correlation functional | static correlation | derivative discontinuity | flat-plane condition | fractional spins

Density functional theory (DFT) (1–3) is now the leading electronic structure method in chemistry, physics, and material science. This success should be attributed to the easily calculated energy functional of 3D electron density, which avoids solving the $3N$-dimensional Schrödinger equation (N being the electron number). Being exact in principle, DFT has to rely on approximations to the unknown exchange-correlation (XC) functional in practical applications. Therefore, better density functional approximations (DFAs) have been the constant pursuit in DFT.

The incorrect treatment of static/strong correlation is among the most challenging problems in DFT (4–6). It is generally recognized that static correlation arises from the (near-)degeneracy of the reference Slater determinant with other low-energy configurations, while dynamic correlation is from the mixing of higher-energy excited configurations. Unlike the short-range feature of dynamic correlation, being multicenter in range (7) makes it difficult to model static correlation with (semi)local functionals.

To understand the systematic errors in existing DFAs and to guide the construction of better approximations, knowledge of the conditions satisfied by the exact functional is essential. Of particular interest here are the exact conditions of DFT on fractional charges and fractional spins. For fractional charges, the Perdew–Parr–Levy–Balduz (PPLB) condition (8–11) requires the total energy, as a function of electron number, to be piecewise straight lines interpolating between adjacent integers. Convex deviation from this piecewise linearity for fractional-charge (FC) systems has been defined as the delocalization error (4, 12, 13), which is related to the earlier concept of many-electron self-interaction error (14–17). For fractional spins, the constancy condition (4, 13, 18) requires the energy of a system with fractional-spin (FS) states to equate that of the comprising degenerate pure-spin states, which is a special case of the conditions for general degenerate states derived in ref. 9. Violation of this constancy requirement is the static correlation error inherent in approximate functionals (18). The FC and FS conditions were unified and extended to a more general and stringent condition, the flat-plane condition (19). The flat-plane condition requires the energy of systems with fractional charges and spins to be two flat planes intersecting in a seam defined by the line of integer electron number. It is this requirement that a discontinuous behavior comes out automatically when total electron number passes through an integer for any fractional spins, revealing the explicitly discontinuous nature of the derivative of the XC functional (19). Its satisfaction requires that the exact XC functional is not a continuously differentiable functional of either the electron density or the (generalized) Kohn–Sham [(G)KS] density matrix for strongly correlated systems (19). In comparison, the derivative discontinuity requirement derived from the PPLB condition for fractional charges is only a subset—it only requires that the exact XC functional is not a continuously differentiable functional of the electron density (20, 21).

The behavior of semilocal functionals exemplified by BLYP (22, 23) is shown in Fig. 1*A*. As can be seen, the correct piecewise flat-plane behavior is erroneously smoothed out into a continuous shape. This poor performance indicates that severe delocalization and static correlation errors exist in the functional, which thus cause the spectacular failures in practical calculations (4, 11–19, 24). In particular, the erroneous dissociation limits of H_2^+ and H_2, resulting, respectively, from the large deviations of the FC point, H $(\frac{1}{2}, 0)$, from linearity and the FS point, H $(\frac{1}{2}, \frac{1}{2})$, from constancy, are simple examples of the delocalization and static correlation errors (4, 13, 18).

Significance

The static correlation error inherent in commonly used density functional approximations (DFAs) has seriously hindered the application of density functional theory (DFT) to strongly correlated systems. Here, an effective fractional-spin correction against the important issue of static/strong correlation in DFT is developed. With this, the flat-plane behavior of various DFAs is largely restored, and the potential energy curves of dissociation of ionic species, single bonds, and multiple bonds are properly described, which demonstrates great improvement in the treatment of strong correlation. This work should have a significant impact on the development and application of DFT.

Author contributions: N.Q.S., C.L., and W.Y. designed research; N.Q.S. performed research; N.Q.S and W.Y. analyzed data; and N.Q.S, C.L., and W.Y. wrote the paper.

The authors declare no conflict of interest.

This article is a PNAS Direct Submission.

[1]To whom correspondence should be addressed. Email: weitao.yang@duke.edu.

This article contains supporting information online at www.pnas.org/lookup/suppl/doi:10.1073/pnas.1807095115/-/DCSupplemental.

Published online September 10, 2018.

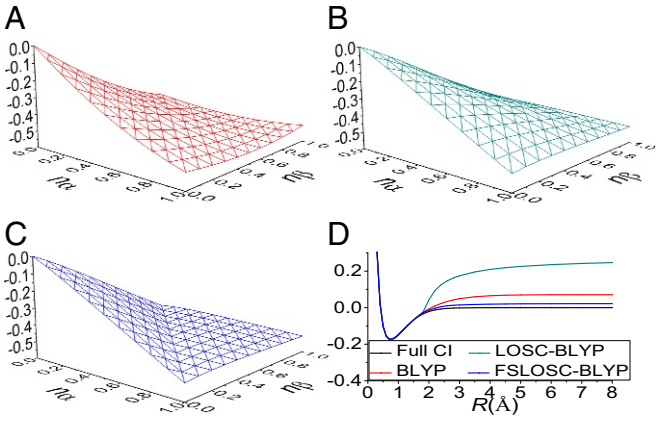

Fig. 1. Total energy of hydrogen atom with fractional charges and fractional spins, H (n^{α}, n^{β}). (*A*–*C*) BLYP (*A*), LOSC-BLYP (*B*), and FSLOSC-BLYP (*C*) are examined. (*D*) Potential energy curve for H–H bond dissociation in H_2. The total energy of two isolated doublet H atoms is set to zero in *D*. All energies are in a.u.

Intensive efforts have been made to eliminate the FC (14–17, 24–55) and FS (7, 18, 24, 26, 50–59) errors. In contrast to the great progresses made to improve the FC-error-related calculations, such as better prediction of ionization potentials and electron affinities (26–33, 46, 48, 52), and proper description of dissociation of cationic species (16, 17, 34, 47–52), etc., the FS error is still an outstanding issue. More precisely, to properly take into account the necessary static correlation without involving multideterminantal reference states remains a major challenge in DFT. Work from Becke showed some promise of describing static correlation with XC hole modeling (7, 60, 61), based on which Johnson and Contreras-García constructed strong-correlation models that improve the description of atoms with fractional charges and spins (58, 59). Recent works on recovering the flat-plane condition include the judiciously modified DFT approach (62) and the density matrix minimization model (63). We aim to develop general corrections to common DFAs by imposing the flat-plane condition on global and local regions, to systematically reduce the delocalization and static correlation errors for mainstream DFAs, all within the (G)KS single-determinant description of the electron density.

In this work, an effective FS correction is developed for the static correlation in DFT. Paired with the FC correction, i.e., the localized orbital scaling correction (LOSC) (48), our model of XC functional takes the form (see *SI Appendix*, section 1 for the expression of the total electronic energy):

$$E_{\mathrm{XC}}[\rho] = E_{\mathrm{XC}}^{\mathrm{DFA}}[\rho] + \Delta E^{\mathrm{FC}}[\rho] + \Delta E^{\mathrm{FS}}[\rho], \qquad [1]$$

where $E_{\mathrm{XC}}^{\mathrm{DFA}}[\rho]$ can be any functional of local density approximation (LDA), generalized gradient approximation (GGA), hybrid GGA, etc. Both spin-restricted and -unrestricted (G)KS methods are available (64, 65). Spin-restricted self-consistent field (SCF) (3, 66, 67) is used here to ensure that the systems possess the correct spin symmetry. In principle, the exact functional can give unrestricted solutions and degenerate restricted solutions which are with integer occupations in closed-shell systems and can be with fractional spins in open-shell systems (18, 19). A restricted solution with integer occupations for open-shell systems is a constrained solution (65) for correct spin symmetry. Before proceeding to derive the FS correction, the FC corrections will be first revisited below.

FC Correction Revisited

The scaling correction (SC) method (46) provides a simple and direct way to fix the incorrect FC behavior of mainstream DFAs. The correction is derived from the energy deviation of each component from linearity to second order, which leads to

$$\Delta E_{\mathrm{CO}}^{\mathrm{FC}} = \sum_{\sigma} \frac{1}{2} n_f^{\sigma}(1 - n_f^{\sigma}) \kappa^{\mathrm{FC}}[\rho_f, \rho_f]. \qquad [2]$$

Here, we assume all canonical orbitals (COs) are occupied by integer (0/1) α and β electrons except orbital f whose occupations are n_f^{α} and n_f^{β}. $\rho_f(\mathbf{r})$ is orbital density $|\varphi_f(\mathbf{r})|^2$; and $\boldsymbol{\kappa}^{\mathrm{FC}}$, here termed FC curvature matrix, takes the form of (with the extension from ref. 48)

$$\kappa^{\mathrm{FC}}[\rho_p, \rho_q] = (1 - d_{\mathrm{X}}^{\mathrm{HF}}) \left[\iint \frac{\rho_p(\mathbf{r})\rho_q(\mathbf{r}')}{|\mathbf{r} - \mathbf{r}'|} d\mathbf{r} d\mathbf{r}' - \frac{2C_{\mathrm{X}}}{3} \int [\rho_p(\mathbf{r})\rho_q(\mathbf{r})]^{2/3} d\mathbf{r} \right], \qquad [3]$$

where $C_{\mathrm{X}} = \frac{3}{4}(\frac{6}{\pi})^{1/3}$, $d_{\mathrm{X}}^{\mathrm{HF}}$ is the amount of HF exchange energy in the parent functional. As only the corrections to the Coulomb and exchange energies were treated in the SC method, Eq. **3** only encompasses curvatures for these two parts. With the integer points kept intact, Eq. **2** mainly restores the linear FC behavior; thus, it greatly improves the prediction of vertical ionization potentials (I_{ve}) and electron affinities (A_{ve}) from energies of the highest occupied molecular orbitals (HOMOs) and the lowest unoccupied molecular orbitals (LUMOs) for small sized systems.

To bring in correction for systems with integer electrons in a size-consistent manner, the local SC (LSC) (47) was proposed by imposing the PPLB condition to local regions of a system. More recently, the LSC scheme was further generalized and LOSC was developed to use localized orbitals (LOs) and LO occupations to capture local FC information in the energy correction (48). LOSC is capable of correcting the total energy and orbital energies in a size-consistent manner; therefore, it improves the descriptions of dissociation of cationic species, the small-sized molecular and polymer band gaps. The LOSC correction to total energy is calculated via

$$\Delta E_{\mathrm{LO}}^{\mathrm{FC}} = \sum_{pq} \sum_{\sigma} \frac{1}{2} \lambda_{pq}^{\sigma}(\delta_{pq} - \lambda_{pq}^{\sigma}) \kappa^{\mathrm{FC}}[\rho_p, \rho_q]. \qquad [4]$$

Here, LOs are obtained by unitary transformation upon COs, $\phi_p(\mathbf{r}) = \sum_q U_{pq}\varphi_q(\mathbf{r})$, with $\boldsymbol{U}$ defining the mixing of COs. The local occupation matrix $\boldsymbol{\lambda}^{\sigma}$ is computed via $\lambda_{pq}^{\sigma} = \langle\phi_p|\rho_s^{\sigma}|\phi_q\rangle$. Each diagonal element, λ_{pp}^{σ}, represents the occupation of an LO. Note that each off-diagonal element, λ_{pq}^{σ}, relates to an LO pair, with the magnitude indicating how much the pair of LOs formed from the mixing of the same occupied COs. $\kappa^{\mathrm{FC}}[\rho_p, \rho_q]$ is the FC curvature associated with LOs, obtained by inserting LO densities, $\rho_p(\mathbf{r}) = |\phi_p(\mathbf{r})|^2$, into Eq. **3**.

The desired LOs are optimized through a special localization procedure (48), with the following objective function

$$F = \sum_{p} \left[\langle\phi_p|\mathbf{r}^2|\phi_p\rangle - \langle\phi_p|\mathbf{r}|\phi_p\rangle^2 \right] + \sum_{pq} \omega_{pq} |\langle\phi_p|\varphi_q\rangle|^2. \qquad [5]$$

Here, the first term is the Foster–Boys objective function for physical space localization (68), while the second term is to restrict the mixing of COs with large energy difference. The LOs so obtained are called orbitalets, with localization in both physical and energy spaces (48). We would like to make comparison of LOSC with existing corrections using LOs, the generalized transition state (GTS) method (69), the LDA+U method (70,

71), and the Fermi–Lowdin orbital self-interaction correction (FLOSIC) (72, 73). GTS improves the LDA calculation for band gaps of solids, with an energy correction of $\Delta E^{\mathrm{GTS}} = \sum_i \frac{1}{2}\kappa_{ii}(\lambda_{ii} - \lambda_{ii}^2)$, where each κ_{ii} is determined by separate constrained LDA calculations. A scheme similar to GTS was recently constructed by Ma and Wang (74). In these works, the LOs come from mixing of only occupied or virtual COs; thus, they do not change the total energies for physical systems with integer number of electrons; hence, these energy functionals are not size consistent (48) and can only correct orbital energies (with failure, e.g., for H_2^+ dissociation). In contrast, LOSC mixes occupied and virtual COs in the localization and offers an explicit form of Eq. **3** for the $\boldsymbol{\kappa}$ matrix. It corrects the DFA energies at both integer and fractional electron numbers. Moreover, Eq. **4** involves off-diagonal κ_{pq} and λ_{pq} that are crucial to dispel the unwanted interaction between LO pairs for the dissociation of cationic species. In the case of H_2^+ dissociation, it is only with these off-diagonal terms that the correct asymptotic behavior as $R \to \infty$ can be retrieved (*SI Appendix*, section 2.B). LDA+U uses a quadratic energy correction, uses transition metal d atomic orbitals as LOs, and determines the U parameters through linear response calculations or empirically. In contrast, LOSC uses the explicit functional form for the curvatures, and the orbitalets are dynamical because of energy localization, in that they can be just the COs as in H_2^+ at equilibrium bond length and become localized like atomic orbitals at dissociation limit. The use of orbitalets allows a different and appropriate amount of corrections to the delocalization error in DFAs at different geometries, which cannot be achieved with a fixed set of atomic orbitals as in LDA+U. In a quite different manner, FLOSIC relies on the elimination of self-interaction for each LO, which spans the occupied space only.

To increase the ability of capturing the delocalization information of reaction transition states, in this work we use a modified ω_{pq} of the form

$$\omega_{pq} = R_0^2\{\exp[|\varepsilon_p - \varepsilon_q|/\varepsilon_0 + \mathrm{erfc}(\eta\sqrt{d_p d_q})] - 1\}, \qquad [6]$$

which depends not only on energy difference of COs, $\varepsilon_p - \varepsilon_q$, but also on the spatial delocalization of two COs, $d_p d_q$. Here, d_p is called orbital delocalization factor, calculated via $d_p = \sum_{A<B} Q_p(A)|\mathbf{R}_A - \mathbf{R}_B|Q_p(B)$, where A and B are atomic indices, $\mathbf{R}_A$ is the atomic position, and $Q_p(A)$ represents how much the p-th CO localized on atom A (*SI Appendix*, section 2.A). Importantly, to capture the local FS information for FS correction, spin restriction is imposed during localization. The three parameters in Eq. **6** are: $R_0 = 4.2\mathring{A}$, $\varepsilon_0 = 20eV$, and $\eta = 3.78\mathring{A}^{-1}$. They are adjusted to obtain a balanced behavior between reaction barrier heights in HTBH38/08 and NHTBH38/08 (75) and the potential energy curve of H_2.

With this choice for ω_{pq}, the mixing between COs whose orbital energies are far apart is suppressed. Furthermore, spatially delocalized COs are more likely to mix with each other, which is conducive to the characterization of transition states, making use of the delocalized nature of these states.

FS Correction

The FC correction with LOSC only restores the linearity condition for fractional charges and largely eliminates the delocalization error in common DFAs. Here, we develop an FS correction to restore the flat-plane condition in DFAs and thus to properly describe the static correlation. We first consider the correction using COs. Based on the energy deviation of each component from the corresponding flat-plane condition, the mixed-spin terms form the CO-based FS correction (*SI Appendix*, section 1.D), taking the following quadratic form

$$\Delta E_{\mathrm{CO}}^{\mathrm{FS}} = -\Lambda(n_f^\alpha, n_f^\beta)\kappa^{\mathrm{FS}}[\rho_f, \rho_f], \qquad [7]$$

with $\Lambda(n_f^\alpha, n_f^\beta)$ defined as

$$\Lambda(n_f^\alpha, n_f^\beta) = \begin{cases} n_f^\alpha n_f^\beta, & n_f^\alpha + n_f^\beta \le 1 \\ (1-n_f^\alpha)(1-n_f^\beta), & n_f^\alpha + n_f^\beta > 1. \end{cases} \qquad [8]$$

Here, the FS curvature matrix, $\boldsymbol{\kappa}^{\mathrm{FS}}$, is calculated by

$$\kappa^{\mathrm{FS}}[\rho_p, \rho_q] = \iint \frac{\rho_p(\mathbf{r})\rho_q(\mathbf{r}')}{|\mathbf{r}-\mathbf{r}'|}\,d\mathbf{r}d\mathbf{r}' + \kappa_{\mathrm{C}}[\sqrt{\rho_p\rho_q}], \qquad [9]$$

where the first term is obtained from the Coulomb energy as a quadratic function of n_f^σ. As the exchange energy is between same-spin electrons, it makes no contribution to the FS correction and curvature. Thus, the main problem is to derive the curvature from the correlation energy, κ_{C}. Here, an approximate κ_{C} has been derived by imposing the constancy condition of fractional spins on the correlation energy (*SI Appendix*, section 1.D), it takes the following general form:

$$\kappa_{\mathrm{C}}[\rho_f] = -4\int \rho_f(\mathbf{r})(\epsilon_{\mathrm{C}}^1[\rho_f] - \epsilon_{\mathrm{C}}^0[\rho_f])\,d\mathbf{r}. \qquad [10]$$

ϵ_{C}^0 and ϵ_{C}^1 are the spin-compensated and fully spin-polarized correlation energy densities. While different kinds of functional approximations can be used in Eq. **10**, the simple LDA forms of ϵ_{C}^0 and ϵ_{C}^1 developed recently (76) are used presently.

Eq. **7** provides the necessary correction for systems with fractional spins, combined with the FC correction of Eq. **2**, a new functional, FS corrected SC (FSSC), can be constructed through

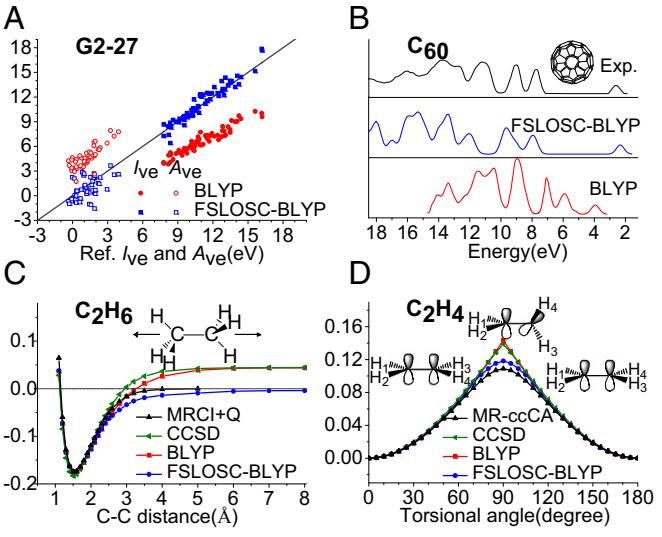

Fig. 2. (*A*) Calculated $-\varepsilon_{\mathrm{HOMO}}$ ($-\varepsilon_{\mathrm{LUMO}}$) vs. reference I_{ve} (A_{ve}) for 64 (47) molecules from the G2-97 set (77). Reference data are obtained by CCSD(T) calculation and extrapolated to infinite basis limit. The solid line indicates $-\epsilon_{\mathrm{HOMO}} = I_{ve}$ or $-\epsilon_{\mathrm{LUMO}} = A_{ve}$. All data in *A* are in electronvolts. (*B*) Spectra of fullerene C_{60} obtained with BLYP and FSLOSC-BLYP, broadened by a 0.25-eV Gaussian, compared with experimental photoemission spectrum (78, 79). (*C*) Potential energy curve for C–C dissociation in C_2H_6. The total energy of two isolated doublet $\cdot CH_3$ is set to zero. MRCI+Q data (80) are used as reference. (*D*) Potential energy curve for twisted ethylene as a function of the HCCH torsion angle (θ). The energy at $\theta = 0$ is set to zero. MR-ccCA data (81) are used as reference. All energies in both *C* and *D* are in a.u.

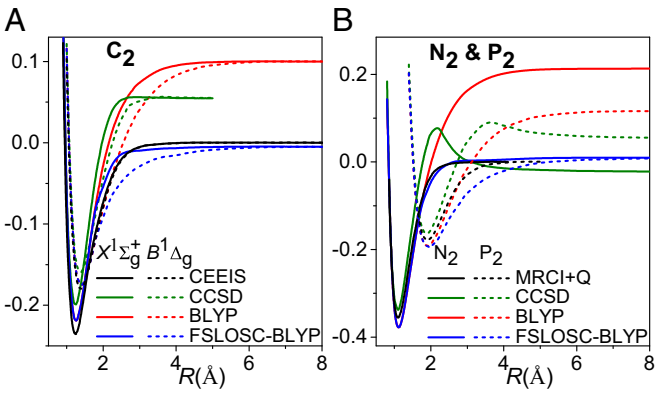

Fig. 3. (*A*) Potential energy curves for C–C bond dissociation in C_2. Two singlet states $X^1\Sigma_g^+$ and $B^1\Delta_g$ are plotted. Data of the correlation energy extrapolation by intrinsic scaling (CEEIS) method (82) are used as reference. The total energy of two triplet C atoms is set to zero. All of the methods show a crossing between $X^1\Sigma_g^+$ and $B^1\Delta_g$ at ∼1.6 Å. (*B*) Potential energy curves for N–N bond dissociation in N_2 and P–P bond dissociation in P_2. The total energies of two quartet N atoms and two quartet P atoms are set to zero for N_2 and P_2, respectively. MRCI+Q data (83) are used as reference. All energies are in a.u.

Eq. **1**. This functional can largely restore the flat-plane behavior, so that it improves the behavior of mainstream DFAs for small-sized systems with fractional charges and spins. However, this functional provides no correction for calculations in physical systems without fractionally occupied COs. To address the issue of static correlation in realistic systems with integer electrons and spins, an effective FS correction based on fractionally occupied LOs should be constructed, as was developed in LOSC (48) for the delocalization error correction.

Similar to the extension of FC correction from Eq. **2** to Eq. **4**, the extension of the FS part can be performed by imposing a correction of Eq. **7** on each LO. The resulting FS correction works well for a system with well-separated fragments, but not for a system with overlapping LOs. Taking chemical-bond breaking as an example, as a bond is gradually stretched, the static correlation effect becomes increasingly pronounced. At the beginning of the dissociation, the bonding orbital (an occupied CO) will mix with the corresponding antibonding orbital (an unoccupied CO) into a pair of overlapping LOs; at this point, the positive correction provided by the FC correction is numerically much larger than the magnitude of the negative correction provided by the FS correction, resulting in a positive overall correction (*SI Appendix*, section 2.D). However, due to the lack of static correlation, the total energy calculated by commonly used DFAs is already too high; thus, the positive FC correction pushes the energy in the wrong direction. Therefore, proper treatment of the interaction between fragments with fractionally occupied LOs is essential for constructing LO-based FS correction. Considering all factors, the final FS correction takes the form

$$\Delta E_{\mathrm{LO}}^{\mathrm{FS}} = -\sum_p \left[(1-S_p)\Lambda(\lambda_{pp}^{\alpha},\lambda_{pp}^{\beta}) + S_p\Gamma(\lambda_{pp}^{\alpha},\lambda_{pp}^{\beta})\right]\kappa^{\mathrm{FS}}[\rho_p,\rho_p] + \sum_{p\neq q}\lambda_{pq}^{\alpha}\lambda_{pq}^{\beta}\kappa^{\mathrm{FS}}[\rho_p,\rho_q], \qquad [11]$$

where $\kappa^{\mathrm{FS}}[\rho_p,\rho_q]$ is the FS curvature matrix defined on LOs, calculated by inserting LO densities into Eq. **9**. When a set of LOs is formed from the mixing of the same COs, S_p defines how much the overlap between the p-th LO and other LOs in the set. S_p approaches 0 when the p-th LO is well-separated from other LOs; otherwise, S_p is large with a maximum of 1. The definition of S_p will be given below.

We now discuss the form of Eq. **11**. The first sum of Eq. **11** is about the correction for each lone LO with fractional spins. In this part, the two terms in brackets correspond to the corrections for well-separated and overlapping LOs, respectively. For a well-separated LO, i.e., $S_p = 0$, only the first term is effective, and this part of correction reduces to a form similar to Eq. **7**, thus providing a correct description for well-separated fragments; for a large S_p, as stated above, the FC correction from Eq. **4** causes a large positive correction that cannot be well neutralized by the first term. To fix this, the second term in the bracket is brought in, where $\Gamma(\lambda_{pp}^{\alpha},\lambda_{pp}^{\beta})$ takes the form of

$$\Gamma(\lambda_{pp}^{\alpha},\lambda_{pp}^{\beta}) = \min(\lambda_{pp}^{\alpha},\lambda_{pp}^{\beta})\min(1-\lambda_{pp}^{\alpha},1-\lambda_{pp}^{\beta}), \qquad [12]$$

which properly compensates for the positive correction from Eq. **4** when S_p is large. Note that for any LO, $\Gamma(\lambda_{pp}^{\alpha},\lambda_{pp}^{\beta})$ is nonzero only when both λ_{pp}^{α} and λ_{pp}^{β} are fractional—thus, it takes effect only for FS cases. The second sum of Eq. **11** is the correction for each mixed-spin LO pair. Similar to the off-diagonal terms in Eq. **4** for correcting asymptotic behavior of the ionic molecule dissociation, this term further corrects the asymptotic behavior for the dissociation of covalent bonds in neutral molecules (*SI Appendix*, section 2).

The foregoing analysis thus suggests that S_p in Eq. **11** should (*i*) allow the use of a set of LOs that are formed from the mixing of the same COs, and (*ii*) evaluate the degree of overlap between the p-th LO and other LOs in the set. As stated above, the off-diagonal element, λ_{pq}^{σ}, indicates how much a pair of LOs formed from the mixing of the same COs. Thus, the set of LOs (including the p-th LO) is formed by those LOs with large $[(\lambda_{pq}^{\alpha})^2+(\lambda_{pq}^{\beta})^2]$. Here, the degree of overlap between the p-th LO and other LOs in the set is evaluated by $S_p = \mathrm{erf}\left(\gamma\left(\int\sqrt{\rho_p(\mathbf{r})\rho_{q_{pmax}}(\mathbf{r})}d\mathbf{r}\right)^{\frac{1}{2}}\right)$, where $q_{pmax} = \mathrm{argmax}_q[(\lambda_{pq}^{\alpha})^2+(\lambda_{pq}^{\beta})^2]$. γ, a parameter for controlling the change of S_p, is set at $\gamma = 1.5$, which was optimized for a smooth dissociation curve for H_2 (*SI Appendix*, Fig. S2).

With the FS correction described above, the new XC functional, the FS-corrected LOSC (FSLOSC), can be constructed. It should be noted that, because of the presence of $\Lambda(\lambda_{pp}^{\alpha},\lambda_{pp}^{\beta})$ and $\Gamma(\lambda_{pp}^{\alpha},\lambda_{pp}^{\beta})$ in the FS correction, the new functional is no longer a continuously differentiable functional of the (G)KS density matrix everywhere, but, rather, a functional encoding the derivative discontinuity, necessary for strongly correlated systems (19).

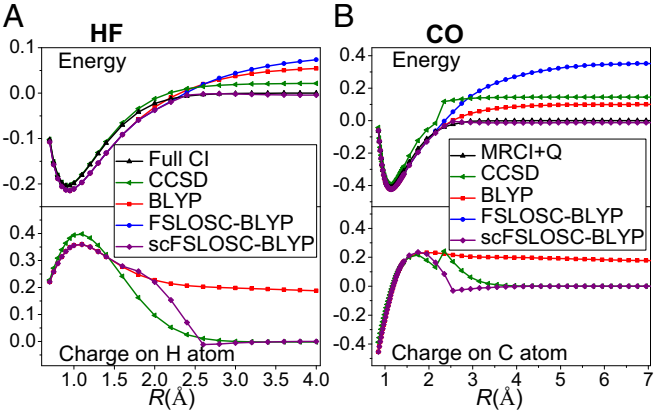

Fig. 4. (*A*) Potential energy curve and charge on H atom along H–F bond dissociation in HF. The total energy of a doublet H atom and a doublet F atom is set to zero. Full CI data (84) are used as reference. (*B*) Potential energy curve and charge on C atom along C–O bond dissociation in CO. The total energy of a triplet C atom and a triplet O atom is set to zero. MRCI+Q data (85) are used as reference. All energies and charges are in a.u.

The orbital energies of FSLOSC can be obtained as

$$\varepsilon_s^{\mathrm{FSLOSC},\sigma} = \langle\varphi_s|h^{\mathrm{FSLOSC},\sigma}|\varphi_s\rangle. \quad [13]$$

Here, the FSLOSC effective Hamiltonian $h^{\mathrm{FSLOSC},\sigma}$ is calculated by $h^{\mathrm{FSLOSC},\sigma} = h^{\mathrm{DFA},\sigma} + \Delta h^{\mathrm{FC},\sigma} + \Delta h^{\mathrm{FS},\sigma}$, with $h^{\mathrm{DFA},\sigma}$ from the parent DFA, $\Delta h^{\mathrm{FC},\sigma}$ from the FC correction (48), and $\Delta h^{\mathrm{FS},\sigma}$ from the FS correction (*SI Appendix*, section 2.F).

FSLOSC calculation can be performed in two ways. One is post-SCF, indicated as FSLOSC-DFA, in which FSLOSC corrections to the total energy and orbital energies are calculated after the SCF calculation of a parent DFA. The second is self-consistent calculation of FSLOSC, i.e., scFSLOSC-DFA. With the FSLOSC effective Hamiltonian, the routine SCF calculation or some gradient optimization algorithm can be applied to obtain a set of optimized orbitals, which improves the energy and density simultaneously. Since the effective Hamiltonian used here is derived based on the frozen-orbital assumption, we used the gradient-based optimization algorithm in combination with line search for better convergence.

Results and Conclusion

FSLOSC is examined on a variety of properties. The tests based on HTBH38/08, NHTBH38/08 (75), and G2-97 (77) test sets indicate that FSLOSC-DFAs show obvious improvement on reaction barrier heights while nearly keeping the thermochemistry unchanged (*SI Appendix*, Tables S1 and S2). In particular, dissociation of molecules without breaking space or spin symmetry is tested, which is one of the most demanding challenges in DFT since it requires a balanced treatment of dynamical and static correlation. In the following, the results of BLYP and (sc)FSLOSC-BLYP will be discussed; CCSD (86–88) results are also included for comparison. More calculation details and test results can be found in *SI Appendix*, section 3.

For the flat-plane test on the H atom, Fig. 1 shows that LOSC has corrected the convex FC behavior of BLYP, but enlarges the FS error. With FS correction, FSLOSC restores the flat-plane behavior, and consequently both dissociation limits of H_2^+ and H_2 are corrected.

In addition to the simple H–H bond breaking in H_2, the excellent description of potential energy curves of σ bond breaking in ethane and π bond breaking in twisted ethene again shows that FSLOSC is able to handle strongly correlated systems without involving multideterminantal reference states; Fig. 2 *C* and *D*. Furthermore, the improved prediction of I_{ve}, A_{ve}, and quasiparticle spectra by orbital energies of FSLOSC demonstrates that the delocalization error is greatly reduced, which is similar to LOSC (48); Fig. 2 *A* and *B*.

Moreover, FSLOSC can correctly dissociate multiple bonds. The dissociation curves of C_2, N_2, and P_2 can be found in Fig. 3. These systems are not only a challenge to DFT, but also to wave-function methods. Because of the lack of static correlation, the CCSD level of correlation method is still insufficient to correctly describe multiple bond breaking. BLYP performs well at equilibrium distance, but its energies become too high as the bonds are stretched. FSLOSC, with the energies of BLYP around equilibrium kept unchanged, repairs the dissociation limits of BLYP, thus yielding good potential energy curves.

It has been found that semilocal DFAs can dramatically underestimate the energy of dissociating neutral heteroatom molecules into fractionally charged fragments in unrestricted (G)KS calculations with broken symmetry (14, 15, 89). The symmetry-preserved restricted calculations of such systems, however, lead to much too high energies at dissociation limits because of static correlation error as shown in FS behavior (18). Here, we test two molecules, single-bond HF and multiple-bond CO; Fig. 4. Restricted BLYP gives too high energies at dissociation limits and incorrectly predicts the charge distribution, showing fractional positive charge on H and C atoms at dissociation limits. Based on this erroneous charge distribution, FSLOSC in post-SCF application cannot improve the energies of BLYP. Through the self-consistent calculations, i.e., scFSLOSC, the charge distributions as well as the energies at dissociation limits are both improved. Therefore, scFSLOSC is necessary when the density of the parent DFA is incorrect.

To conclude, an effective FS correction has been developed to restore the flat-plane behavior and correct the static correlation error in existing DFAs. Based on this, the FSLOSC functional developed in this work shows significant improvement in the treatment of strongly correlated systems. All of the tests demonstrate that FSLOSC greatly reduces the delocalization and static correlation errors in mainstream DFAs.

ACKNOWLEDGMENTS. This work was supported by the Center for Computational Design of Functional Layered Materials, an Energy Frontier Research Center funded by the US Department of Energy, Office of Science, Basic Energy Sciences (Award DE-SC0012575, to N.Q.S.); National Institutes of Health Grant R01 GM061870-13 (to W.Y.); and National Science Foundation Grant CHE-1362927 (to C.L.).

1. Hohenberg P, Kohn W (1964) Inhomogeneous electron gas. *Phys Rev* 136:B864–B871.
2. Kohn W, Sham LJ (1965) Self-consistent equations including exchange and correlation effects. *Phys Rev* 140:A1133–A1138.
3. Parr RG, Yang W (1989) *Density-Functional Theory of Atoms and Molecules* (Oxford Univ Press, New York).
4. Cohen AJ, Mori-Sánchez P, Yang W (2012) Challenges for density functional theory. *Chem Rev* 112:289–320.
5. Burke K (2012) Perspective on density functional theory. *J Chem Phys* 136:150901.
6. Becke AD (2014) Perspective: Fifty years of density-functional theory in chemical physics. *J Chem Phys* 140:18A301.
7. Becke AD (2013) Density functionals for static, dynamical, and strong correlation. *J Chem Phys* 138:074109.
8. Perdew JP, Parr RG, Levy M, Balduz JL (1982) Density-functional theory for fractional particle number: Derivative discontinuities of the energy. *Phys Rev Lett* 49:1691–1694.
9. Yang W, Zhang Y, Ayers PW (2000) Degenerate ground states and a fractional number of electrons in density and reduced density matrix functional theory. *Phys Rev Lett* 84:5172–5175.
10. Zhang Y, Yang W (2000) Perspective on "density-functional theory for fractional particle number: Derivative discontinuities of the energy". *Theor Chem Acc* 103:346–348.
11. Perdew JP, et al. (2007) Exchange and correlation in open systems of fluctuating electron number. *Phys Rev A* 76:040501.
12. Mori-Sánchez P, Cohen AJ, Yang W (2008) Localization and delocalization errors in density functional theory and implications for band-gap prediction. *Phys Rev Lett* 100:146401.
13. Cohen AJ, Mori-Sánchez P, Yang W (2008) Insights into current limitations of density functional theory. *Science* 321:792–794.
14. Mori-Sánchez P, Cohen AJ, Yang W (2006) Many-electron self-interaction error in approximate density functionals. *J Chem Phys* 125:201102.
15. Ruzsinszky A, Perdew JP, Csonka GI, Vydrov OA, Scuseria GE (2006) Spurious fractional charge on dissociated atoms: Pervasive and resilient self-interaction error of common density functionals. *J Chem Phys* 125:194112.
16. Ruzsinszky A, Perdew JP, Csonka GI, Vydrov OA, Scuseria GE (2007) Density functionals that are one- and two- are not always many-electron self-interaction-free, as shown for H_2^+, He_2^+, LiH^+, and Ne_2^+. *J Chem Phys* 126:104102.
17. Vydrov OA, Scuseria GE, Perdew JP (2007) Tests of functionals for systems with fractional electron number. *J Chem Phys* 126:154109.
18. Cohen AJ, Mori-Sánchez P, Yang W (2008) Fractional spins and static correlation error in density functional theory. *J Chem Phys* 129:121104.
19. Mori-Sánchez P, Cohen AJ, Yang W (2009) Discontinuous nature of the exchange-correlation functional in strongly correlated systems. *Phys Rev Lett* 102: 066403.
20. Perdew JP, Levy M (1983) Physical content of the exact Kohn-Sham orbital energies: Band gaps and derivative discontinuities. *Phys Rev Lett* 51:1884–1887.
21. Sham LJ, Schlüter M (1983) Density-functional theory of the energy gap. *Phys Rev Lett* 51:1888–1891.
22. Becke AD (1988) Density-functional exchange-energy approximation with correct asymptotic-behavior. *Phys Rev A* 38:3098–3100.
23. Lee C, Yang W, Parr RG (1988) Development of the Colle-Salvetti correlation-energy formula into a functional of the electron density. *Phys Rev B* 37:789.
24. Haunschild R, Henderson TM, Jiménez-Hoyos CA, Scuseria GE (2010) Many-electron self-interaction and spin polarization errors in local hybrid density functionals. *J Chem Phys* 133:134116.

25. Cohen AJ, Mori-Sánchez P, Yang W (2007) Development of exchange-correlation functionals with minimal many-electron self-interaction error. *J Chem Phys* 126:191109.
26. Cohen AJ, Mori-Sánchez P, Yang W (2009) Second-order perturbation theory with fractional charges and fractional spins. *J Chem Theor Comput* 5:786–792.
27. Su NQ, Xu X (2015) Integration approach at the second-order perturbation theory: Applications to ionization potential and electron affinity calculations. *J Chem Theor Comput* 11:4677–4688.
28. Su NQ, Xu X (2016) Second-order perturbation theory for fractional occupation systems: Applications to ionization potential and electron affinity calculations. *J Chem Theor Comput* 12:2285–2297.
29. Stein T, Autschbach J, Govind N, Kronik L, Baer R (2012) Curvature and frontier orbital energies in density functional theory. *J Phys Chem Lett* 3:3740–3744.
30. Tsuneda T, Song JW, Suzuki S, Hirao K (2010) On Koopmans' theorem in density functional theory. *J Chem Phys* 133:174101.
31. Dabo I, et al. (2010) Koopmans' condition for density-functional theory. *Phys Rev B* 82:115121.
32. Su NQ, Yang W, Mori-Sánchez P, Xu X (2014) Fractional charge behavior and band gap predictions with the xyg3 type of doubly hybrid density functionals. *J Phys Chem A* 118:9201–9211.
33. Kraisler E, Kronik L (2013) Piecewise linearity of approximate density functionals revisited: Implications for frontier orbital energies. *Phys Rev Lett* 110:126403.
34. Kraisler E, Kronik L (2015) Elimination of the asymptotic fractional dissociation problem in Kohn-Sham density-functional theory using the ensemble-generalization approach. *Phys Rev A* 91:032504.
35. Cococcioni M, de Gironcoli S (2005) Linear response approach to the calculation of the effective interaction parameters in the LDA + U method. *Phys Rev B* 71:035105.
36. Kulik H, Cococcioni M, Scherlis D, Marzari N (2006) Density functional theory in transition-metal chemistry: A self-consistent Hubbard U approach. *Phys Rev Lett* 97:103001.
37. Lany S, Zunger A (2009) Polaronic hole localization and multiple hole binding of acceptors in oxide wide-gap semiconductors. *Phys Rev B* 80:085202.
38. Baer R, Livshits E, Salzner U (2010) Tuned range-separated hybrids in density functional theory. *Annu Rev Phys Chem* 61:85–109.
39. Salzner U, Baer R (2009) Koopmans' springs to life. *J Chem Phys* 131:231101.
40. Gaiduk A, Firaha D, Staroverov V (2012) Improved electronic excitation energies from shape-corrected semilocal Kohn-Sham potentials. *Phys Rev Lett* 108:253005.
41. Srebro M, Autschbach J (2012) Does a molecule-specific density functional give an accurate electron density? The challenging case of the CuCl electric field gradient. *J Phys Chem Lett* 3:576–581.
42. Refaely-Abramson S, et al. (2012) Quasiparticle spectra from a nonempirical optimally tuned range-separated hybrid density functional. *Phys Rev Lett* 109:226405.
43. Malek A, Peng D, Yang W, Balawender R, Holas A (2014) Testing exchange–correlation functionals at fractional electron numbers. *Theor Chem Acc* 133:1559.
44. Hellgren M, Rohr DR, Gross EKU (2012) Correlation potentials for molecular bond dissociation within the self-consistent random phase approximation. *J Chem Phys* 136:034106.
45. Hellgren M, et al. (2015) Static correlation and electron localization in molecular dimers from the self-consistent RPA and *gw* approximation. *Phys Rev B* 91:165110.
46. Zheng X, Cohen A, Mori-Sánchez P, Hu X, Yang W (2011) Improving band gap prediction in density functional theory from molecules to solids. *Phys Rev Lett* 107:026403.
47. Li C, Zheng X, Cohen AJ, Mori-Sánchez P, Yang W (2015) Local scaling correction for reducing delocalization error in density functional approximations. *Phys Rev Lett* 114:053001.
48. Li C, Zheng X, Su NQ, Yang W (2017) Localized orbital scaling correction for systematic elimination of delocalization error in density functional approximations. *National Sci Rev* 5:203–215.
49. Bao JL, Gagliardi L, Truhlar DG Self-interaction error in density functional theory: An appraisal. *J Phys Chem Lett* 9:2353–2358.
50. Mori-Sánchez P, Cohen AJ, Yang W (2012) Failure of the random-phase-approximation correlation energy. *Phys Rev A* 85:042507.
51. van Aggelen H, Yang Y, Yang W (2013) Exchange-correlation energy from pairing matrix fluctuation and the particle-particle random-phase approximation. *Phys Rev A* 88:030501.
52. Steinmann SN, Yang W (2013) Wave function methods for fractional electrons. *J Chem Phys* 139:074107.
53. Phillips JJ, Kananenka AA, Zgid D (2015) Fractional charge and spin errors in self-consistent Green's function theory. *J Chem Phys* 142:194108.
54. Nafziger J, Wasserman A (2015) Fragment-based treatment of delocalization and static correlation errors in density-functional theory. *J Chem Phys* 143:234105.
55. Mussard B, Toulouse J (2017) Fractional-charge and fractional-spin errors in range-separated density-functional theory. *Mol Phys* 115:161–173.
56. Filatov M (2015) Spin-restricted ensemble-referenced Kohn–Sham method: Basic principles and application to strongly correlated ground and excited states of molecules. *Wiley Interdiscip Rev Comput Mol Sci* 5:146–167.
57. Kong J, Proynov E (2016) Density functional model for nondynamic and strong correlation. *J Chem Theor Comput* 12:133–143.
58. Johnson ER, Contreras-García J (2011) Communication: A density functional with accurate fractional-charge and fractional-spin behaviour for s-electrons. *J Chem Phys* 135:081103.
59. Johnson ER (2013) A density functional for strong correlation in atoms. *J Chem Phys* 139:074110.
60. Becke AD (2003) A real-space model of nondynamical correlation. *J Chem Phys* 119:2972–2977.
61. Becke AD (2005) Real-space post-Hartree–Fock correlation models. *J Chem Phys* 122:064101.
62. Bajaj A, Janet JP, Kulik HJ (2017) Communication: Recovering the flat-plane condition in electronic structure theory at semi-local DFT cost. *J Chem Phys* 147: 191101.
63. Zhou F, Ozolins V (2017) A unified treatment of derivative discontinuity, delocalization and static correlation effects in density functional calculations. arXiv: 1710.08973.
64. Seidl A, Görling A, Vogl P, Majewski JA, Levy M (1996) Generalized Kohn-Sham schemes and the band-gap problem. *Phys Rev B* 53:3764–3774.
65. Jacob CR, Reiher M (2012) Spin in density-functional theory. *Int J Quantum Chem* 112:3661–3684.
66. Roothaan CCJ (1960) Self-consistent field theory for open shells of electronic systems. *Rev Mod Phys* 32:179–185.
67. Filatov M, Shaik S (1998) Spin-restricted density functional approach to the open-shell problem. *Chem Phys Lett* 288:689–697.
68. Foster JM, Boys SF (1960) Canonical configurational interaction procedure. *Rev Mod Phys* 32:300–302.
69. Anisimov VI, Kozhevnikov AV (2005) Transition state method and Wannier functions. *Phys Rev B* 72:075125.
70. Himmetoglu B, Floris A, Gironcoli S, Cococcioni M (2014) Hubbard-corrected DFT energy functionals: The LDA+U description of correlated systems. *Int J Quantum Chem* 114:14–49.
71. Kulik HJ (2015) Perspective: Treating electron over-delocalization with the DFT+U method. *J Chem Phys* 142:240901.
72. Pederson MR, Ruzsinszky A, Perdew JP (2014) Communication: Self-interaction correction with unitary invariance in density functional theory. *J Chem Phys* 140:121103.
73. Yang Zh, Pederson MR, Perdew JP (2017) Full self-consistency in the fermi-orbital self-interaction correction. *Phys Rev A* 95:052505.
74. Ma J, Wang LW (2016) Using Wannier functions to improve solid band gap predictions in density functional theory. *Sci Rep* 6:24924.
75. Peverati R, Truhlar DG (2014) Quest for a universal density functional: The accuracy of density functionals across a broad spectrum of databases in chemistry and physics. *Philos Trans A Math Phys Eng Sci.* 372:20120476.
76. Chachiyo T (2016) Communication: Simple and accurate uniform electron gas correlation energy for the full range of densities. *J Chem Phys* 145:021101.
77. Curtiss LA, Raghavachari K, Redfern PC, Pople JA (1997) Assessment of Gaussian-2 and density functional theories for the computation of enthalpies of formation. *J Chem Phys* 106:1063–1079.
78. Liebsch T, et al. (1996) Photoelectron spectroscopy of free fullerenes. *J Electron Spectros Relat Phenomena* 79:419–422.
79. Blase X, Attaccalite C, Olevano V (2011) First-principles *GW* calculations for fullerenes, porphyrins, phtalocyanine, and other molecules of interest for organic photovoltaic applications. *Phys Rev B* 83:115103.
80. Li C, Evangelista FA (2017) Driven similarity renormalization group: Third-order multireference perturbation theory. *J Chem Phys* 146:124132.
81. Jiang W, Jeffrey CC, Wilson AK (2012) Empirical correction of nondynamical correlation energy for density functionals. *J Phys Chem A* 116:9969–9978.
82. Boschen JS, Theis D, Ruedenberg K, Windus TL (2013) Accurate ab initio potential energy curves and spectroscopic properties of the four lowest singlet states of C_2. *Theor Chem Acc* 133:1425.
83. Xu LT, Dunning TH (2015) Generalized valence bond description of the ground states ($x_1\sigma_g^+$) of homonuclear pnictogen diatomic molecules: N_2, P_2, and As_2. *J Chem Theor Comput* 11:2496–2507.
84. Dutta A, Sherrill CD (2003) Full configuration interaction potential energy curves for breaking bonds to hydrogen: An assessment of single-reference correlation methods. *J Chem Phys* 118:1610–1619.
85. Shi DH, Li WT, Sun JF, Zhu ZL (2013) Theoretical study of spectroscopic and molecular properties of several low-lying electronic states of co molecule. *Int J Quan Chem* 113:934–942.
86. Čížek J (1969) *Advances in Chemical Physics*, edited by Hariharan PC (Wiley Interscience, New York), Vol 14, p 35.
87. Purvis GD III, Bartlett RJ (1982) A full coupled-cluster singles and doubles model - The inclusion of disconnected triples. *J Chem Phys* 76:1918.
88. Pople JA, Head-Gordon M, Raghavachari K (1987) Quadratic configuration interaction—a general technique for determining electron correlation energies. *J Chem Phys* 87:5975.
89. Zhang Y, Yang W (1998) A challenge for density functionals: Self-interaction error increases for systems with a noninteger number of electrons. *J Chem Phys* 109:2604–2608.